Ablation dynamics in wire array Z-pinches under modifications on global magnetic field topology

Felipe Veloso, Gonzalo Muñoz-Cordovez, Luis Donoso-Tapia, Vicente Valenzuela-Villaseca, Francisco Suzuki-Vidal, George Swadling, Jeremy Chittenden, Mario Favre, and Edmund Wyndham

Citation: Physics of Plasmas **22**, 072509 (2015); doi: 10.1063/1.4926581
View online: http://dx.doi.org/10.1063/1.4926581
View Table of Contents: http://scitation.aip.org/content/aip/journal/pop/22/7?ver=pdfcov
Published by the AIP Publishing

Ablation dynamics in wire array Z-pinches under modifications on global magnetic field topology

Felipe Veloso,[1,a)] Gonzalo Muñoz-Cordovez,[1] Luis Donoso-Tapia,[1] Vicente Valenzuela-Villaseca,[1] Francisco Suzuki-Vidal,[2] George Swadling,[2] Jeremy Chittenden,[2] Mario Favre,[1] and Edmund Wyndham[1]
[1]*Instituto de Física, Pontificia Universidad Católica de Chile, Av Vicuña Mackenna 4860, Macul, Santiago, Chile*
[2]*Blackett Laboratory, Imperial College, London SW7 2BW, United Kingdom*

(Received 7 April 2015; accepted 25 June 2015; published online 14 July 2015)

The dynamics of ablation streams and precursor plasma in cylindrical wire array Z-pinches under temporal variations of the global magnetic field topology is investigated through experiments and numerical simulations. The wire arrays in these experiments are modified by replacing a pair of consecutive wires with wires of a larger diameter. This modification leads to two separate effects, both of which impact the dynamics of the precursor plasma; firstly, current is unevenly distributed between the wires and secondly, the thicker wires take longer to fully ablate. The uneven distribution of current is evidenced in the experiments by the drift of the precursor off axis due to a variation in the global magnetic field topology which modifies the direction of the ablation streams tracking the precursor position. The variation of the global magnetic field due to the presence of thick wires is studied with three-dimensional magnetohydrodynamic (MHD) simulations, showing that the global field changes from the expected toroidal field to a temporally variable topology after breakages appear in the thin wires. This leads to an observed acceleration of the precursor column towards the region closer to the thick wires and later, when thick wires also present breakages, it continues moving away from the original array position as a complicated and disperse object subject to MHD instabilities [http://dx.doi.org/10.1063/1.4926581]

I. INTRODUCTION

Wire array Z-pinches are efficient and powerful X-ray sources. They are also used in a variety of research areas, such as inertial confinement fusion, laboratory astrophysics, radiation science, and high energy density studies among others.[1–6] These arrays are composed of several fine metallic wires cylindrically arranged as load of a pulsed power driver, where fast rising electrical currents above 100's kA in 100's ns turn them into plasma and drive them according to the global Lorentz $\mathbf{J} \times \mathbf{B}$ force. It is well known that the dynamics of wire array plasmas does not follow a shell-like implosion. Instead, it evolves through a gradual implosion of the low density coronal plasma produced from wire ablation that surrounds the solid wire core (known as core-corona structures). These wire cores remain at their initial position providing material to the coronal plasma, which is continuously driven away from the wires by the $\mathbf{J} \times \mathbf{B}$ force acting on it.[7]

The ablation dynamics in wire array z-pinches is dominated by the global magnetic field of the configuration, which is particular to its specific topology. In wire-based z-pinch plasmas (such as cylindrical, inverse, conical, or planar wire array configurations), the global magnetic field is the superposition of the local magnetic fields around each wire that composes the array. This global field, which "surrounds" the entire wire array, drives the ablated plasma perpendicular to it towards the region where this field is zero.[8–10] In cylindrical wire arrays with fixed wire material and wire diameter (referred to as "standard arrays" from now onwards), some interesting features have been reported as a consequence of the presence of the global field. In particular, once the ablation streams from the wires have developed, they present axial modulations with a typical wavelength dependent on the wire material ($\lambda \sim 0.5$ mm for Al, $\lambda \sim 0.25$ mm for W), which is a consequence of the global field topology that swept the coronal plasma accumulated in the vicinity of the wires away from them.[11,12] Furthermore, it has been found that these streams can be narrowed by the field penetration within the array and its curvature close to each wire.[13] The ablation dynamics in wire arrays is not only important because of their influence on the implosion, as it determinates the x-ray emission from these configurations[1,6,14] but also is interesting object to study collisionality processes in dense magnetized supersonic plasma flows. These are relevant as comparable environments for astrophysical processes.[15–17]

Due to the azimuthal symmetry imposed on standard arrays, the ablation flows from each wire radially converge toward the array axis, where plasma accumulates forming a precursor plasma column. Even after most of the wires have been fully ablated and during the implosion phase as well, the null field region (and consequently, the precursor) remains at the array axis. However, some standard array configurations have shown displacement of the precursor off the array axis and the effects of this displacement were studied mainly concerning how it affects the x-ray pulse at stagnation. In these cases, the displacement was achieved

a)fveloso@fis.puc.cl

unintentionally due to asymmetries on the current distribution within the array produced by modifications on the generator parameters, such as changes on the load return current path[18,19] or asynchronous actuation of the different modules of the pulsed power device.[20] In this paper, the effects of non-axially symmetric temporal variations of the magnetic field topology on the ablation phase and on the ablation streams in wire arrays dynamics are investigated. By using different wire diameters of the same material within the array, the proportion of the total current flowing through each wire is modified due to the differences of the inductance presented by wires of differing diameters. This produces an uneven distribution of the current among different wires which results in the modification of the global magnetic field of the configuration from the azimuthally symmetric topology of the standard arrays. Moreover, at later times of the discharge other dynamic effects appear on the current distribution (and consequently, on plasma dynamics) principally due to the different characteristic times for full ablation of the wires. Hence at later times in the discharge, the dense cores of thinner wires present breakages earlier when compared to the thicker ones. This in turn causes changes in the value of the equivalent impedance of the wires and therefore, on the global field topology as well.

II. EXPERIMENTAL SETUP AND IMAGING DIAGNOSTICS

The experiments were performed using the Llampudken generator,[21] which delivers a peak current of ~350 kA in ~350 ns as measured with an integrated Rogowski coil, as shown in Figure 1(a). The wire arrays were mounted as loads for the generator with a length of 23 mm and an 8 mm diameter. The experiments used either tungsten or aluminium as the wire material on each array. The wires were equally spaced in an axisymmetrical cylindrical configuration similar to a standard array, but replacing a pair of consecutive wires with wires of a larger diameter in comparison to the rest. The wires had the same mass ratio, 1:6, in all the experiments, by using 10 μm and 25 μm diameter wires. The resistive effects produced by the use of different wire diameters in the load should be important before breakdown occurs along the wires. Since ~1 kA/wire is needed for breakdown, the influence of different resistances should impact on the energy deposited on the solid wires mainly during the first ~10 ns of the discharge, until the very low resistivity coronal plasma conducts the greater part of the current.[22,23] In any case, the resolution of the electrical diagnostics is limited by the use of an integrator circuit for the Rogowski coil and the level of electrical noise at very early times. On the contrary, during most of discharge, it can be assumed that the load current is divided on the wires based on their self-inductance ratio considering them as parallel inductors for the load. Considering this, it is reasonable to estimate that the two thick wires each carry nearly 12% more current than each thin wire producing an uneven current distribution within the wire array. For the experiments described here, eight wires were used for tungsten arrays, whereas aluminum experiments used four wires. Schematic diagrams of the arrays are shown in Figures 1(b) and 1(c). If these arrays were compared to standard arrays, they would represent a mass per unit length similar to eight wires of 15 μm each for W (~28 μg/m) and 10 wires of 12 μm each for Al (~3 μg/m). These values mean that the equivalent tungsten configuration would be overmassed, whereas the equivalent aluminium configuration would have an implosion time close to peak current. Hence, for the experiments described in this paper, it is expected to observe more significant effects of the variations of magnetic field topology in the aluminium configuration than that with tungsten arrays.

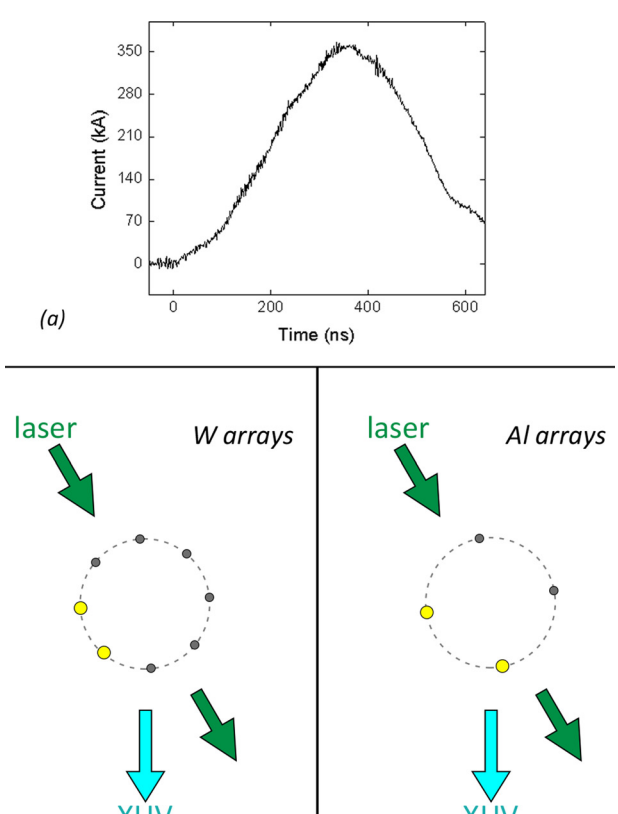

FIG. 1. (a) Experimental current trace. (b) and (c) End-on schematic view of wire arrays indicating the approximate lines-of-sight of the diagnostics (green: laser beam, light blue: XUV imaging). Thicker wires are represented using yellow dots, whereas thinner wires use gray dots. (a) 6 × 10 μm + 2 × 25 μm W wires and (b) 2 × 10 μm + 2 × 25 μm Al wires.

The plasma dynamics is diagnosed using side-on (i.e., perpendicular to the axis between electrodes) time-resolved laser probing and extreme ultraviolet (XUV) self-emission imaging. Laser shadowgraphy is performed using a frequency doubled Nd:YAG laser (532 nm, 12 ps) and recorded using open-shutter DSLR cameras with interference filters at the laser wavelength. Pinhole XUV imaging of the plasma self-emission is achieved using two 2-frame micro-channel plate cameras (MCP) with ~5 ns temporal resolution. Pinhole diameters of 100 μm are used without any filtering. These MCPs are positioned to observe thicker wires on the edge of the array. A rough diagram of the orientation of the arrays with respect to the diagnostics lines-of-sight is shown in Figures 1(b) and 1(c).

III. RESULTS AND DISCUSSION

A. Tungsten wire array experiments

At the beginning of the discharge (200 ns), the results indicate that any differences of the global magnetic field in the configuration are minimal and almost undetectable in comparison to the standard cylindrical wire array configuration, i.e., the null magnetic field region should be located close to the array axis. This situation is observed in tungsten experiments as the plasma precursor appears very near the array axis, as shown in the shadowgraphy images of Figure 2(a). The precursor appears hollow in this diagnostic at 200 ns and the later development of an m = 1 magnetohydrodynamic (MHD) instability suggests that current is flowing through it. It is also observed that the ablation streams from thinner wires can be seen extending toward to the array axis, which is not the case for thicker wires. It is important to emphasize that shadowgraphy is sensitive to variations on the density gradients, which means that the absence of ablation streams in the images coming from thick wires does not necessarily indicate there are no streams coming out from them. As a matter of fact, it is likely that these streams are indeed present, but they do not have large enough spatial variations in density to be observed with this probing technique. Figure 2(a) also shows that plasma streams at later times (437 ns) do not appear to be directed towards the array axis. Instead, they seem to have a velocity component not directed radially, instead towards the thicker wires side of the array (as indicated by a red arrow). A plausible explanation for this effect is that ablation streams coming out from the wires are changing their direction from purely radial to that towards a region close to the thicker wires. Since at early times (200 ns), the precursor is formed on axis and the ablation streams are heading to it, and later (437 ns), the plasma ablates elsewhere, it can be concluded that the global magnetic field topology is changing in time, in accordance to the net $\mathbf{J} \times \mathbf{B}$ force. In addition, the self-emission image shown in Figure 2(b) shows more emission from the zone close to thicker wires in comparison to the opposite side of the array, which can be an indicator of more light emitting sources at that region (i.e., more plasma). Therefore, these observations show that plasma is not only accumulating on axis but also an important fraction of it is accumulating in the region closer to thicker wires. Hence, the ablation streams from these wires are probably embedded in a diluted background of plasma which is not the case for the opposite side of the array. All of these results indicate that throughout the discharge, the current is being redistributed unevenly along different diameter wires, along the precursor plasma (as observed from the m = 1 instability) and, possible, along the diluted background plasma as well.

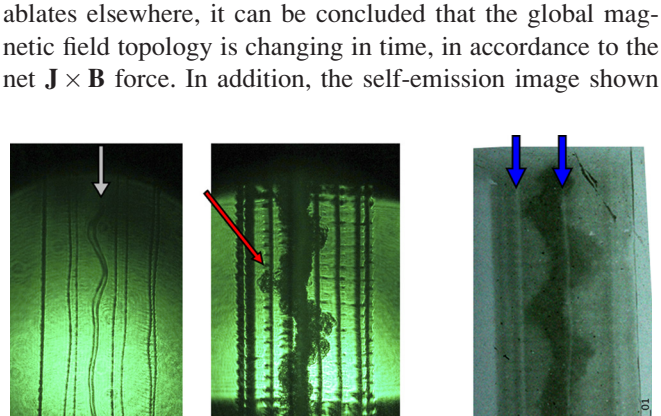

FIG. 2. Experimental results from tungsten arrays (6 × 10 μm + 2 × 25 μm wires). (a) Optical laser shadowgraphy and (b) XUV self-emission. Yellow arrows indicate the position of the thicker wires. In (a), the gray arrow at 200 ns indicates the position of the precursor plasma column, whereas the red arrow at 437 ns indicates ablation streams moving toward thicker wires position. Blue arrows in (b) indicate wire cores due to precursor backlighting.

The orientation of the array with respect to the imaging XUV diagnostics also allows recording the backlighting of the wire cores by the self-emission from the plasma, resulting in wire core diameters of ~0.2–0.25 mm for a thick wire and ~0.1–0.15 mm for a thin wire (blue arrows in Fig. 2(b)). Unfortunately, higher resolution images are required to measure the core sizes in more detail. This could be achieved by using an X-pinch backlighting source instead. Nevertheless, it is clear that the proportion of wire core sizes remains similar to the original wire diameter throughout the discharge. If different wires expand in the same proportion, this indicates that ablation rates are not strongly affected by the ~12% difference on current flowing through thick and thin wires.

B. Aluminium wire array experiments

In contrast to tungsten experiments, the aluminium arrays have a mass per unit length comparable to the optimal for reaching imploding conditions on the Llampudken generator and they use only four wires instead of eight. Even though the differences on the number of wires within the array could modify the narrowing of the ablation streams,[13] experiments using four wires in standard wire array configurations have shown similar imploding dynamics to those performed using eight (or more) wires in standard arrays.[24] As a result, the effects of reducing the number of wires do not affect the ablation dynamics as importantly as using different wire diameters within the array. Therefore, the effects of using the appropriate mass per unit length for the generator should produce much more evident differences on the plasma dynamics due to the magnetic field topology variations than the overmassed experiments. As observed from laser probing results in Figure 3(a), from early times in the discharge (~200 ns), the plasma ablated from the wires accumulates near the symmetry axis, but slightly shifted towards the side of the thicker wires (almost hidden by a thick wire). Similar to the tungsten experiments, the precursor plasma also exhibits what appears to be m = 1 instabilities from early times. These instabilities on the precursor are either developed earlier in time or they have a faster growth rate when compared to previously reported standard array experiments driven at the Llampudken generator and using similar mass per unit length in the load.[25] This comparison indicates that even though both configurations are cylindrical arrays with similar mass in the load, the current distributes

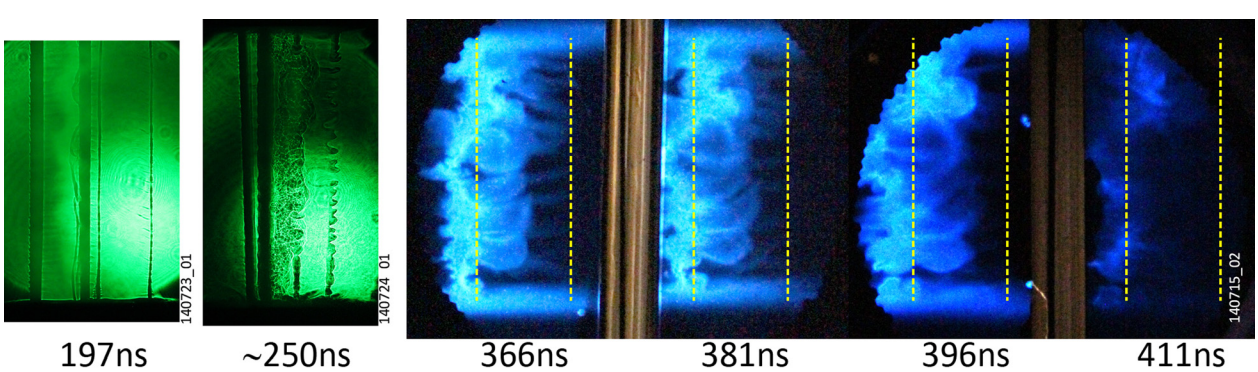

FIG. 3. Experimental results using aluminium arrays ($2 \times 10\,\mu m + 2 \times 25\,\mu m$ wires). (a) Optical laser shadowgraphy (two different shots). (b) XUV self-emission (from the same shot). In the latter, vertical dashed yellow lines indicate the initial position of edge wires.

differently amongst both the wires and the precursor due to the modified current distribution imposed from early times in the discharge by the variation in the impedance of the load wires within the array. Figure 3(a) shows wire breakage on the thinner wires occurs at ~250 ns and the plasma being swept away from the wires towards a "diffuse" precursor plasma shifted to the position of the thicker wires of the array. At this time, the precursor and the remaining thicker wires should carry most of the current since they provide a continuous path between cathode and anode. Since the precursor does not have a solid core or a fixed position in space, it gains momentum directed towards the gap produced in the inter-wires space increasing its mass from the ablation of the remaining thicker wires. These effects cause the precursor plasma to move outside the region delimited by the positions of the wires in the array as shown in the XUV images of Figure 3(b). From these results, a characteristic velocity of the precursor column can be estimated. The precursor is observed to move from the axis to the array boundary during the time interval of ~190 ns to 366 ns, from which the average plasma velocity can be estimated as $\sim 3 \times 10^4$ m/s. This value is similar to measurements done using tungsten wires in a 16 mm configuration previously reported in Ref. 26. It is worthwhile mentioning that this characteristic velocity is not necessarily uniform along the precursor due to the development of instabilities (MHD or others) along the plasma column.

C. Numerical simulations

The variation of the magnetic field topology may be studied by simulating the experiments using the 3D resistive magnetohydrodynamics code GORGON.[27] This code has proved to be a robust and accurate tool for Z-pinch modelling. A central portion of the each array of 7 mm height has been simulated using a Cartesian grid with a spatial resolution of 30 μm on each dimension. Figure 4 shows 2D maps of mass density in two different planes: in the x-z plane that passes through diametrically opposed wires in the array, and in the x-y plane similar to the end-on probing diagram shown in Figure 1. The x-y maps are taken after averaging the 3D simulations along the z-axis. In addition, isocontours of the magnetic field are also included. In both cases (Al and W), the simulations describe some of the features discussed previously regarding the variations on the field topology due to different wire sizes within the array. It can be observed that the local field lines around the thicker wires enclose a slightly larger area than those enclosing the thinner wires, even before the appearance of breaks in the thinner wires. This is caused by the higher proportion of the current flowing through them, as expected from the differences in self-inductances previously discussed. As a result, the global field inside the array does not have the cylindrical symmetry expected from a standard array configuration, which affects the dynamics of the plasma accumulating in the precursor as well. The plasma ablated from the wires does not necessarily stagnate on axis, but spreads over the inner region of the array closer to the thicker wires. This situation has been experimentally observed in the backlighting of the wire cores observed in only the side closer to thick wires of the array discussed for tungsten arrays.

Even though the ablation streams and precursor dynamics are affected from early times in the discharge compared to standard arrays, the most significant effects are produced when thinner wires present breakages along their length. This occurs at ~220–230 ns for Al arrays, and at ~440–450 ns for W. These discontinuities produced by the appearance of breakages in thinner wires increase their equivalent impedance as compared to the rest of the array causing significant modifications in the current distribution which are clearly observed in the isocontours of the magnetic field. When the thinner wires have been mostly ablated, the global field outside of the array modifies its shape surrounding both the thicker wires and the precursor plasma. In the tungsten configuration, the thick wires do not present discontinuities on their cores throughout the discharge, probably due to the excess of mass in the load. In this case, the plasma disperses mostly in the quadrant where thick wires are located and the higher density region of the precursor is no longer at the array axis but slightly shifted towards the thick wires position. The ablation streams also show a perceptible angular displacement from a purely radial implosion to coincide with the precursor in its new position. From the magnetic field isocontours, it can also be observed that the disperse precursor carries a fraction of the total current similar to the remaining wires. On the other hand, the mass of the

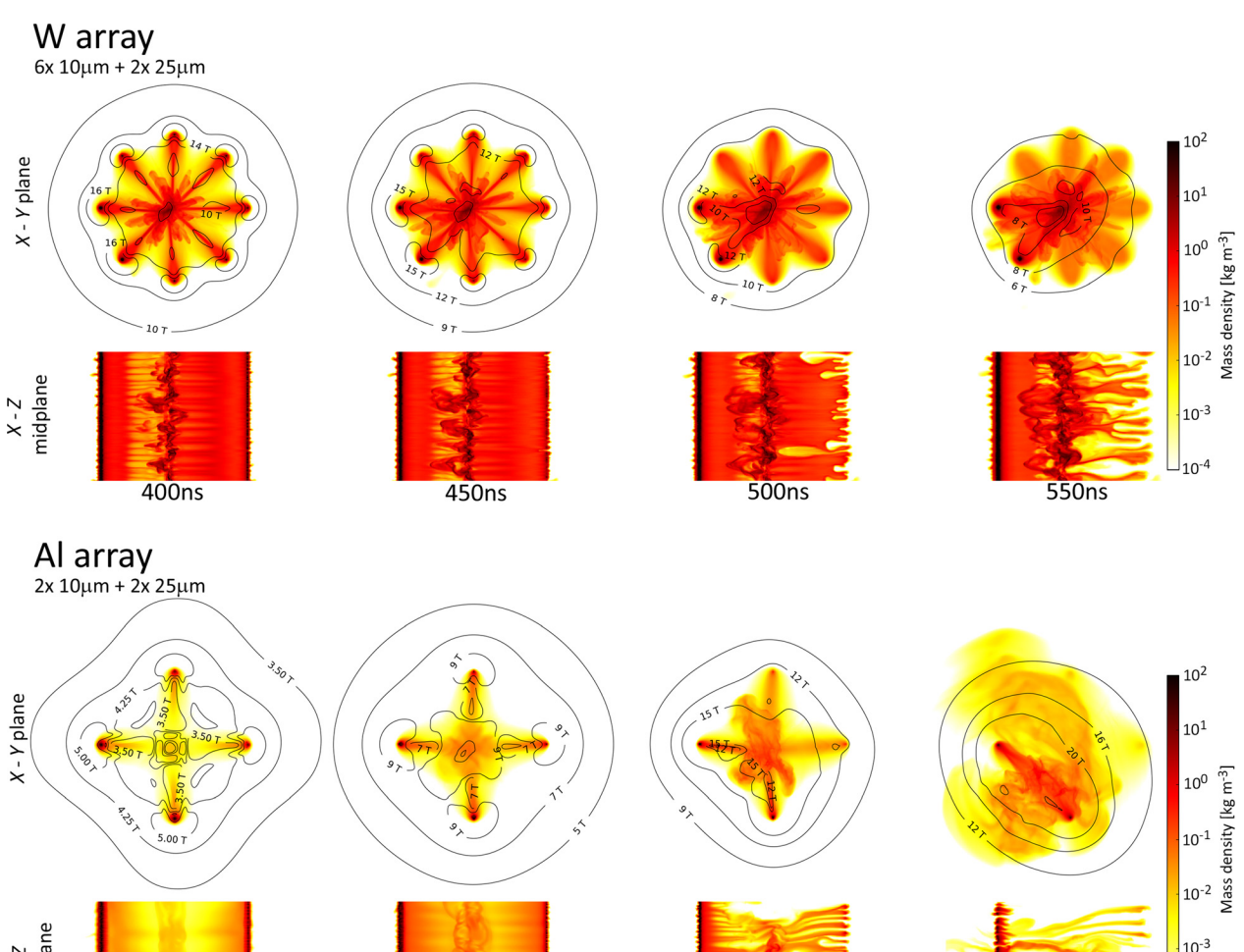

FIG. 4. Mass density plots after GORGON simulations of tungsten (top) and aluminium (bottom) experiments. The x-z plots correspond to the plane defined by diametrically opposed thick and thin wire. Isocontours of the magnetic field in the plane are indicated in x-y plane.

load in the aluminium configuration is considerably lower than the tungsten case and the effects of using different wire diameters within the array are more substantial. For example, when discontinuities appear in the thin wires at ~220–230 ns, the current is still increasing and the precursor displaces its position toward the inter-wire gap between the thicker wires. At later times, the ablated plasma from the wires modifies its direction from purely radially imploding streams to a trajectory that follows the precursor position which is, in turn, gaining momentum towards the midpoint of the plane defined by thick wires. This is in agreement with the experimental observations. At later times ($t > 320$ ns), the field topology is similar to a planar wire array and breakages also appear in the thick wires. In these circumstances, the current is mostly flowing through an unstructured precursor which is already moving in the direction normal to the plane towards the outside of the original array diameter.

IV. FINAL REMARKS

Experiments have been performed in which a standard cylindrical wire array z-pinch is modified by introducing two consecutive thicker wires of the same material, with the aim of studying their effect on the ablation dynamics, precursor formation, and variation of the global magnetic field. All these factors should in principle affect the implosion of the array and the x-ray yield in higher current machines. The temporal variation of the magnetic field topology produces considerable variations in the plasma dynamics, as observed in both experiments and simulations. The ablation streams from the wires change their direction during the discharge and the precursor plasma moves towards the region where the thick wires are located. When the mass per unit length of the load is not as high as an overmassed configuration, the precursor displaces significantly from the array axis and it moves toward the inter-wire gap of thicker wires and beyond with a characteristic velocity of $\sim 3 \times 10^4$ m/s. In addition, previous experiments with standard aluminium arrays performed in the Llampudken generator using a similar mass per unit length as that of the aluminium experiments reported here, the precursor temperature has been estimated in the range 30–50 eV.[24] However, in the experiments where the magnetic field topology changes in time, the precursor plasma is not stationary on axis, hence it is expected to have a temperature closer to the minimum estimation. Assuming a

plasma temperature of 30 eV (lower estimated value for standard aluminium arrays), an average ionization state of 8, a characteristic length scale of $L \sim 1$ mm (i.e., of the order of precursor diameter), and considering transverse Spitzer resistivity, the Reynolds number has a high value ($Re > 10^5$) and the magnetic Reynolds number is $Re_m \sim 1.5$. This indicates that the movement of the plasma is more likely to produce turbulences and that both magnetic diffusion and advection are similarly important on the global magnetic field dynamics with characteristic timescales (L/v) on the order of ~30 ns. The temporal variation of the magnetic field might also induce the triggering of magnetic reconnections within the plasma, but in the present situation, it is not possible to either confirm or discard this possibility. Magnetic probing techniques (such as Faraday rotation) or fast particle detection could help to clarify this issue, but these measurements are beyond the scope of this paper. The study of the ablation dynamics under temporally variable magnetic field topologies can also be used as diagnostic tool for unexpected current distributions and it opens the possibility to study current carrying plasma outflows from cylindrical arrays where different regimes can be studied. Particle emission potentially produced by the changes in field topology, together with precursor dynamics out of the array and its possible interaction with obstacles will be subjects for future studies.

ACKNOWLEDGMENTS

This work has been supported by Fondecyt/Iniciacion 11121621. G. Muñoz-Cordovez and L. Donoso-Tapia acknowledge financial support of CONICYT scholarship for graduate studies.

[1]C. Deeney *et al.*, Phys. Rev. Lett. **81**, 4883 (1998).
[2]T. W. L. Sanford *et al.*, Phys. Rev. Lett. **77**, 5063 (1996).
[3]J. H. Hammer *et al.*, Phys. Plasmas **6**, 2129 (1999).
[4]M. E. Cuneo *et al.*, Phys. Rev. Lett. **88**, 215004 (2002).
[5]J. E. Bailey *et al.*, J. Quant. Spectrosc. Radiat. Transfer **71**, 157 (2001).
[6]J. E. Bailey *et al.*, Phys. Plasmas **9**, 2186 (2002).
[7]S. V. Lebedev, F. N. Beg, S. N. Bland, J. P. Chittenden, A. E. Dangor, M. G. Haines, S. A. Pikuz, and T. A. Shelkovenko, Phys. Rev. Lett. **85**, 98 (2000).
[8]A. J. Harvey-Thompson, S. V. Lebedev, S. N. Bland, J. P. Chittenden, G. N. Hall, A. Marocchino, F. Suzuki-Vidal, S. C. Bott, J. B. A. Palmer, and C. Ning, Phys. Plasmas **16**, 022701 (2009).
[9]D. J. Ampleford *et al.*, Phys. Plasmas **14**, 102704 (2007).
[10]V. V. Ivanov, V. I. Sotnikov, A. Haboub, G. E. Sarkisov, R. Presura, and T. E. Cowan, Phys. Plasmas **14**, 032703 (2007).
[11]J. P. Chittenden and C. A. Jennings, Phys. Rev. Lett. **101**, 055005 (2008).
[12]P. F. Knapp, J. B. Greenly, P. A. Gourdain, C. L. Hoyt, M. R. Martin, S. A. Pikuz, C. E. Seyler, T. A. Shelkovenko, and D. A. Hammer, Phys. Plasmas **17**, 012704 (2010).
[13]I. C. Blesener, J. B. Greenly, B. R. Kusse, K. S. Blesener, C. E. Seyler, and D. A. Hammer, Phys. Plasmas **19**, 022109 (2012).
[14]C. Deeney *et al.*, Phys. Rev. E **56**, 5945 (1997).
[15]G. F. Swadling, S. V. Lebedev, G. N. Hall, F. Suzuki-Vidal, G. Burdiak, A. J. Harvey-Thompson, S. N. Bland, P. De Grouchy, E. Khoory, L. Pickworth, J. Skidmore, and L. Suttle, Phys. Plasmas **20**, 062706 (2013).
[16]G. F. Swadling, S. V. Ledebev, N. Niasse, J. P. Chittenden, G. N. Hall, F. Suzuki-Vidal, G. Burdiak, A. J. Harvey-Thompson, S. N. Bland, P. De Grouchy, E. Khoory, L. Pickworth, and L. Suttle, Phys. Plasmas **20**, 022705 (2013).
[17]G. F. Swadling, S. V. Lebedev, A. J. Harvey-Thompson, W. Rozmus, G. C. Burdiak, L. Suttle, S. Patarkar, R. A. Smith, M. Bennett, G. N. Hall, F. Suzuki-Vidal, and J. Yuan, Phys. Rev. Lett. **113**, 035003 (2014).
[18]S. V. Lebedev, D. J. Ampleford, S. N. Bland, S. C. Bott, J. P. Chittenden, C. Jennings, M. G. Haines, J. B. A. Palmer, and J. Rapley, Nucl. Fusion **44**, S215 (2004).
[19]G. F. Swadling, G. N. Hall, S. V. Lebedev, G. C. Burdiak, F. Suzuki-Vidal, P. de Grouchy, L. Suttle, M. Bennett, and L. Sheng, IEEE Trans. Plasma Sci. **PP**, 1 (2015).
[20]K. N. Mitrofanov, V. V. Aleksandrov, E. V. Grabovski, A. N. Gritsuk, G. M. Oleinik, I. N. Frolov, Ya. N. Laukhin, and A. A. Samokhin, Plasma Phys. Rep. **40**, 323 (2014).
[21]H. Chuaqui, E. Wyndham, C. Friedli, and M. Favre, Laser Part. Beams **15**, 241 (1997).
[22]D. B. Sinars, M. Hu, K. M. Chandler, T. A. Shelkovenko, S. A. Pikuz, J. B. Greenly, D. A. Hammer, and B. R. Kusse, Phys. Plasmas **8**, 216 (2001).
[23]P. U. Duselis, J. A. Vaughan, and B. R. Kusse, Phys. Plasmas **11**, 4025 (2004).
[24]T. A. Shelkovenko, S. A. Pikuz, J. D. Douglass, I. C. Blesener, J. B. Greenly, R. D. McBride, D. A. Hammer, and B. R. Kusse, Phys. Plasmas **14**, 102702 (2007).
[25]F. Veloso, F. Suzuki-Vidal, F. Molina, I. H. Mitchell, H. Chuaqui, M. Favre, and E. Wyndham, IEEE Trans. Plasma Sci. **40**, 3319 (2012).
[26]F. Veloso, L. Donoso, G. Swadling, J. Chittenden, G. Muñoz, V. Valenzuela, F. Suzuki-Vidal, M. Favre, and E. Wyndham, J. Phys.: Conf. Ser. **591**, 012027 (2015).
[27]J. P. Chittenden, S. V. Lebedev, C. A. Jennings, S. N. Bland, and A. Ciardi, Plasma Phys. Controlled Fusion **46**, B457 (2004).